$K^0\Lambda$ and $D^-\Lambda_c^+$ production induced by pion beams off the nucleon

Sang-Ho Kim,[1,*] Hyun-Chul Kim,[2,3,†] and Atsushi Hosaka[4,5,‡]

[1]*Asia Pacific Center for Theoretical Physics (APCTP), Pohang, Gyeongbuk 790-784, Republic of Korea*
[2]*Department of Physics, Inha University, Incheon 402-751, Republic of Korea*
[3]*School of Physics, Korea Institute for Advanced Study (KIAS), Seoul 130-722, Republic of Korea*
[4]*Research Center for Nuclear Physics (RCNP), Osaka University, Ibaraki, Osaka 567-0047, Japan*
[5]*J-PARC Branch, KEK Theory Center, Institute of Particle and Nuclear Studies, KEK, Tokai, Ibaraki 319-1106, Japan*

(Received 23 August 2016; published 21 November 2016)

We present a comparative study on the pion induced production of $K^0\Lambda$ and $D^-\Lambda_c^+$ off the nucleon. A hybrid framework is utilized by combining an effective Lagrangian method with a Regge approach. We consider the t-channel process in a planar diagram by vector-meson Reggeon exchanges and the u-channel one in a nonplanar diagram by baryon Reggeon exchanges. The present model reproduces the $K^0\Lambda$ production data well with a few parameters. Having fixed them, we predict the $D^-\Lambda_c^+$ production, which turns out to be about 10^4–10^6 times smaller than the strangeness one, depending on the kinematical regions.

DOI: 10.1103/PhysRevD.94.094025

I. INTRODUCTION

Experimental findings of new heavy hadrons have renewed great interest in heavy-quark physics (see, for example, reviews [1–4]). For example, the Belle collaboration, *BABAR* collaboration, BESIII collaboration, and LHCb collaboration have reported new types of heavy mesons [5–15]. Moreover, a new bottom baryon $\Xi_b^0(5945)$ has been observed by the CMS collaboration [16], and two new bottom baryon resonances $\Xi_b'(5935)$ and $\Xi_b^*(5955)$ have been announced by the LHCb collaboration [17]. Recently, a new proposal was submitted to Japan Proton Accelerator Research Complex (J-PARC) to measure the production of charmed hadrons. The high-momentum pion beam line up to 20 GeV will be constructed to produce excited charmed baryons [18,19]. The $\pi^- p \to D^{*-}\Lambda_c^+$ reaction was suggested as the first experiment and the relevant theoretical works have been discussed recently by us in collaboration with other authors [20,21]. Reference [20] estimated the production rates of charmed baryons Y_c^+ in the process $\pi^- p \to D^{*-}Y_c^+$, where Y_c^+ is the Λ_c^+, Σ_c^+ and their excited states, with the help of the quark-diquark model. Reference [21] has predicted the magnitude of the total cross section of the $\pi^- p \to D^{*-}\Lambda_c^+$ in comparison with the process of its strangeness partner $\pi^- p \to K^{*0}\Lambda$ based on an effective Lagrangian method and a hybridized Regge model.

In the present work, we aim at a comparative study on the pion-induced production of $K^0\Lambda$ and $D^-\Lambda_c^+$ off the nucleon, as was done for the reaction $\pi^- p \to D^{*-}\Lambda_c^+$ together with the $\pi^- p \to K^{*0}\Lambda$ [21]. In Ref. [21], it was shown that the total cross section for the charm production turned out to be about 10^3–10^6 times smaller than that for the strangeness production, depending on theoretical approaches and kinematical regions. Thus, it is of great interest to investigate whether the $\pi^- p \to D^-\Lambda_c^+$ reaction would show similar features in comparison with those of the $\pi^- p \to K^0\Lambda$. We first consider the $\pi^- p \to K^0\Lambda$ reaction for which the experimental data are known. Since we aim at comparing this reaction with the $\pi^- p \to D^-\Lambda_c^+$, we will mainly concentrate on the features of both reactions at higher energies, where the Regge method comes into essential play. As for the threshold behavior of the $\pi^- p \to K^0\Lambda$, we refer, for example, to Ref. [22] in which a dynamical coupled-channel formalism was used to explain the experimental data near threshold. Then, we will investigate the $\pi^- p \to D^-\Lambda_c^+$ reaction, comparing it with the $\pi^- p \to K^0\Lambda$.

We fix the parameters such as coupling constants and scale factors, using the experimental data on the $\pi^- p \to K^0\Lambda$. Since the amplitudes for the charm production $\pi^- p \to D^-\Lambda_c^+$ have exactly the same structure as the $\pi^- p \to K^0\Lambda$ reaction, we can easily carry out the comparative study, the parameters being assumed to be the same as the strangeness case. We also examine the sensitivity of the results to the changes of the parameters. To fix the Regge parameters such as Regge trajectories and energy scale parameters, we use the nonperturbative quark-gluon string model (QGSM) developed by Kaidalov *et al.* [23–26] as was done in Ref. [21]. We find that the $D\Lambda_c^+$ ($K\Lambda$) production is governed by vector-meson D^* (K^*) Reggeon exchange at forward angles, whereas by baryon Σ_c (Σ) Reggeon exchange at backward angles. We compare the production cross sections for the $\pi^- p \to D^-\Lambda_c^+$ with other models [27,28].

*sangho.kim@apctp.org
†hchkim@inha.ac.kr
‡hosaka@rcnp.osaka-u.ac.jp

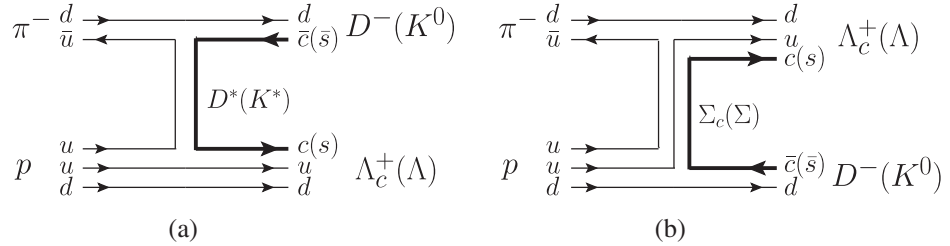

FIG. 1. (a) Planar and (b) nonplanar diagrams for the $\pi^- p \to D^- \Lambda_c^+(K^0\Lambda)$ reaction.

The present work is organized as follows: In the next section, we explain the general formalism of the hybridized Regge model and fix model parameters such as the coupling constants, Regge trajectories and energy scale parameters, and the scale factors. In Sec. III, we show the numerical results and compare them with those from other models. The last section is devoted to the summary and conclusion.

II. GENERAL FORMALISM

We start with explaining a hybridized Regge model combining with an effective Lagrangian method. In general, there are two different diagrams for both reactions $\pi^- p \to D^- \Lambda_c^+$ and $\pi^- p \to K^0 \Lambda$ as drawn in Fig. 1. Vector Reggeon exchange can be understood as a planar diagram, so that the corresponding Regge parameters can be determined explicitly by employing the QGSM [23–26]. On the other hand, the u-channel diagram for $\Sigma_c(\Sigma)$ Reggeon exchange is a nonplanar diagram for which there is no theoretical ground on fixing the parameters. Thus, we will utilize relevant phenomenologies to determine them. The incoming momenta of the pion and the proton are designated respectively by k_1 and p_1, and the outcoming momenta of the pseudoscalar meson and the $\Lambda_c(\Lambda)$ by k_2 and p_2, respectively. We first investigate the strangeness production $\pi^- p \to K^0\Lambda$ with the Regge parameters fixed. Then we will extend the same method to the charm production $\pi^- p \to D^-\Lambda_c^+$.

A. Strangeness production $\pi^- p \to K^0\Lambda$: K^* Reggeon exchange

The K^*-exchange amplitude for the $\pi^- p \to K^0\Lambda$ reaction is derived, based on the effective Lagrangians given as

$$\mathcal{L}_{\pi KK^*} = -ig_{\pi KK^*}(\bar{K}\partial^\mu \boldsymbol{\tau}\cdot\boldsymbol{\pi}K^*_\mu - \bar{K}^*_\mu \partial^\mu \boldsymbol{\tau}\cdot\boldsymbol{\pi}K),$$
$$\mathcal{L}_{K^*N\Lambda} = -g_{K^*N\Lambda}\bar{N}\left[\gamma_\mu\Lambda - \frac{\kappa_{K^*N\Lambda}}{M_N + M_\Lambda}\sigma_{\mu\nu}\Lambda\partial^\nu\right]K^{*\mu} + \text{H.c.}, \tag{1}$$

where π, K, and K^* denote the fields corresponding to the $\pi(140, 0^-)$, $K(494, 0^-)$, and $K^*(892, 1^-)$ mesons respectively, while N and Λ stand for the nucleon and $\Lambda(1116, 1/2^+)$ hyperon, respectively. The coupling constant $g_{\pi KK^*}$ is calculated by using the experimental data on the decay width $\Gamma(K^* \to K\pi)$ [29]: $g_{\pi KK^*} = 6.56$, whereas the $K^*N\Lambda$ coupling can be taken from the Nijmegen soft-core potential (NSC97a) [30]

$$g_{K^*N\Lambda} = -4.26, \qquad \kappa_{K^*N\Lambda} = 2.91. \tag{2}$$

To derive the t-channel Regge amplitude, we employ a hybridized approach by replacing the Feynman propagator for the vector-meson exchange in the t channel with the Regge propagator arising from the corresponding Regge trajectory [21,31]

$$T_{K^*}(s,t) = C_{K^*}(t)\mathcal{M}_{K^*}(s,t)\left(\frac{s}{s^{\pi N:K\Lambda}_{K^*}}\right)^{\alpha_{K^*}(t)-1} \times \Gamma(1-\alpha_{K^*}(t))\alpha_{K^*}{}'. \tag{3}$$

In doing so, we need to examine the behavior of the amplitude in the high-energy region, which will be discussed later. The amplitude $\mathcal{M}_{K^*}$ in Eq. (3) without the propagator is obtained from the Lagrangians in Eq. (1),

$$\mathcal{M}_{K^*}(s,t) = g_{\pi KK^*}g_{K^*N\Lambda}\bar{u}_\Lambda k_1^\mu\left[-g_{\mu\nu} + \frac{q_{t\mu}q_{t\nu}}{M^2_{K^*}}\right] \times \left[\gamma^\nu - \frac{i\kappa_{K^*N\Lambda}}{M_N + M_\Lambda}\sigma^{\nu\lambda}q_{t\lambda}\right]u_N, \tag{4}$$

where u_N and u_Λ stand for the Dirac spinors of the initial nucleon and the final Λ, respectively. The momentum transfer in the t channel is defined as $q_t = k_2 - k_1$. Note that the $q_t^\mu q_t^\nu$ term in Eq. (4) provides a certain contribution, which is distinguished from K^* exchange in $K^+\Lambda$ photoproduction $\gamma p \to K^+\Lambda$ [32] and $\pi^- p \to K^{*0}\Lambda$ [21] reaction in which there is no contribution from it. This is due to the fact that the antisymmetric tensor $\epsilon^{\mu\rho\alpha\beta}q_{t\rho}$ involved in the relevant Lagrangians for K^* exchange eliminates the $q_{t\mu}q_{t\nu}$ term by contraction. The $C_{K^*}(t)$ represents a scale factor [21], which is defined as

$$C_{K^*}(t) = \frac{a_t}{(1 - t/\Lambda^2)^2}. \tag{5}$$

It plays the role of a form factor that reflects a finite size of hadrons. We choose $\Lambda = 1$ GeV and the parameter a_t is determined by the experimental data at high energies: $a_t = 0.40$.

The differential cross section $d\sigma/dt$ is expressed as

$$\frac{d\sigma}{dt} = \frac{1}{64\pi (p_{\text{c.m.}})^2 s} \frac{1}{2} \sum_{s_i, s_f} |T|^2, \tag{6}$$

where $p_{\text{c.m.}}$ denotes the pion momentum in the center-of-mass (c.m.) frame and the nucleon and Λ spins correspond to the s_i and s_f, respectively. Since the Regge amplitudes have a unique virtue that they can describe consistently the diffractive pattern both at forward and backward angles as well as the asymptotic behavior with the unitarity preserved, $d\sigma/dt$ in Eq. (6) should comply with the following asymptotic behavior:

$$\frac{d\sigma}{dt}(s \to \infty, t \to 0) \propto s^{2\alpha(t)-2}. \tag{7}$$

The asymptotic behavior of $\mathcal{M}_{K^*}(s,t)$ is derived as

$$\lim_{s\to\infty} \sum_{s_i, s_f} |\mathcal{M}_{K^*}(s,t)|^2 \propto s^2, \tag{8}$$

which produces a correct asymptotic behavior of the Regge amplitude. Note that Eq. (8) is independent of t, which indicates that the amplitude does not change when $t \to 0$.

It is of great interest to compare the asymptotic behavior of the present Regge amplitude with those of other reactions such as $\gamma N \to K\Lambda$ [32] and $\pi N \to K^*\Lambda$ [21]. In these cases, the amplitudes with vector-meson exchange include the antisymmetric tensor that greatly reduces the amplitudes at very forward angles. Explicitly, $\mathcal{M}_{K^*}$ for these two reactions behaves as

$$\lim_{s\to\infty} \sum_{s_i, s_f} |\mathcal{M}_{K^*}(\gamma N \to K\Lambda, \pi N \to K^*\Lambda)|^2 \propto s^2 t, \tag{9}$$

which is very much distinguished from the present reaction, which has the behavior of Eq. (8).

To obtain the K^*-meson trajectory in Eq. (3), we follow Ref. [33] in which the so-called "square-root" trajectory is used,

$$\alpha(t) = \alpha(0) + \gamma[\sqrt{T} - \sqrt{T - t}], \tag{10}$$

where γ is the universal slope and T the scale parameter being different for each trajectory. Equation (10) can be approximated to a linear form,

$$\alpha(t) = \alpha(0) + \alpha' t, \tag{11}$$

TABLE I. The vector-meson trajectories in the strangeness sector [33,34].

	$\alpha(0)$	$\sqrt{T}$	α' [GeV^{-2}]
$\bar{q}q(\rho)$	0.55	2.46	0.742
$\bar{s}q(K^*)$	0.414	2.58	0.707
$\bar{s}s(\phi)$	0.27	2.70	0.675

in the limit $-t \ll T$ with the slope $\alpha' = \gamma/2\sqrt{T}$. In Ref. [33], the values of γ and $\sqrt{T}$ were determined in the case of the ρ Reggeon as follows:

$$\gamma = 3.65 \pm 0.05 \text{ GeV}^{-1},$$
$$\sqrt{T_\rho} = 2.46 \pm 0.03 \text{ GeV}. \tag{12}$$

Following this method, we are able to find the corresponding value of $\sqrt{T}$ for the K^*-meson trajectory. The additivities of intercepts and of inverse slopes are given as [23,24]

$$2\alpha_{\bar{s}q}(0) = \alpha_{\bar{q}q}(0) + \alpha_{\bar{s}s}(0),$$
$$2/\alpha'_{\bar{s}q} = 1/\alpha'_{\bar{q}q} + 1/\alpha'_{\bar{s}s}, \tag{13}$$

where the $\alpha_{\bar{q}q}(t)$, $\alpha_{\bar{s}q}(t)$, and $\alpha_{\bar{s}s}(t)$ are the trajectories corresponding to ρ, K^*, and ϕ mesons, respectively. Thus, using Eq. (13), we can find the values of $\alpha(0)$, $\sqrt{T}$ and α' for the ϕ trajectory. We summarize the parameters obtained for the vector-meson trajectories in Table I [33,34].

Once we know all the parameters for the vector-meson Regge trajectories, we can easily derive the energy scale parameter $s_{K^*}^{\pi N:K\Lambda}$ in Eq. (3) [23,24]:

$$(s_{K^*}^{\pi N:K\Lambda})^{2(\alpha_{K^*}(0)-1)} = (s^{\pi N})^{\alpha_\rho(0)-1} \times (s^{K\Lambda})^{\alpha_\phi(0)-1}. \tag{14}$$

Using the QGSM [23,24], we find the scale parameters $s^{\pi N}$ and $s^{K\Lambda}$: $s^{\pi N} \simeq 1.5$ GeV^2 and $s^{K\Lambda} \simeq 1.76$ GeV^2. Thus, $s_{K^*}^{\pi N:K\Lambda}$ is obtained as $s_{K^*}^{\pi N:K\Lambda} \simeq 1.66$ GeV^2 by Eq. (14). Note that the t-channel energy scale parameter $s_{K^*}^{\pi N:K\Lambda}$ is the same as that of $s_{K^*}^{\pi N:K^*\Lambda}$ given in the reaction $\pi N \to K^*\Lambda$ [21], because of the same flavor content, $s^{K\Lambda} = s^{K^*\Lambda}$.

B. Strangeness production $\pi^- p \to K^0\Lambda$: Σ Reggeon exchange

We now turn to the nonplanar diagram in Fig. 1(b). Though the vector-meson Reggeon exchange contributes to the amplitude dominantly, baryon exchange also comes into play in describing the experimental data at backward angles. The effective Lagrangians for the Σ exchange are given as

$$\mathcal{L}_{KN\Sigma} = \frac{g_{KN\Sigma}}{M_N + M_\Sigma}\bar{N}\gamma^\mu\gamma_5\boldsymbol{\tau}\cdot\Sigma\partial_\mu K + \text{H.c.},$$
$$\mathcal{L}_{\pi\Sigma\Lambda} = \frac{g_{\pi\Sigma\Lambda}}{M_\Lambda + M_\Sigma}\bar{\Lambda}\gamma^\mu\gamma_5\partial_\mu\boldsymbol{\pi}\cdot\Sigma + \text{H.c.}, \quad (15)$$

where Σ represents the lowest-lying $\Sigma(1190, 1/2^+)$ hyperon. The coupling constants $g_{KN\Sigma}$ and $g_{\pi\Sigma\Lambda}$ are taken from the Nijmegen model (NSC97a) [30]:

$$g_{KN\Sigma} = 4.09, \qquad g_{\pi\Sigma\Lambda} = 11.9. \quad (16)$$

As done in the t-channel Reggeon exchange, we can construct the u-channel Regge amplitude [21],

$$T_\Sigma(s,u) = C_\Sigma(u)\mathcal{M}_\Sigma(s,u)\left(\frac{s}{s_\Sigma^{\pi N:K\Lambda}}\right)^{\alpha_\Sigma(u)-\frac{1}{2}} \times\Gamma\left(\frac{1}{2}-\alpha_\Sigma(u)\right)\alpha'_\Sigma, \quad (17)$$

where $C_\Sigma(u)$ is the scale factor in the u channel, defined as

$$C_\Sigma(u) = \frac{a_u}{(1-u/\Lambda^2)^2}. \quad (18)$$

To avoid ambiguity, we use the same value of the cutoff mass Λ as in the t channel. The parameter a_u is fitted to the experimental data: $a_u = 2.00$. The amplitude $\mathcal{M}_\Sigma$ is written as

$$\mathcal{M}_\Sigma(s,u) = g_{\pi\Sigma\Lambda}g_{KN\Sigma}\bar{u}_\Lambda(\not{q}_u - M_\Sigma)u_N, \quad (19)$$

where q_u denotes the momentum transfer in the u channel, expressed as $q_u = p_2 - k_1$.

The u-channel amplitude should obey the following asymptotic behavior:

$$\frac{d\sigma}{du}(s\to\infty, u\to 0) \propto s^{2\alpha(u)-2}. \quad (20)$$

The unpolarized sum of the squared amplitude in Eq. (19) is shown to be proportional to s, as $s\to\infty$,

$$\lim_{s\to\infty}\sum_{s_i,s_f}|\mathcal{M}_\Sigma(s,u)|^2 \propto s, \quad (21)$$

which satisfies the general asymptotic behavior of the Regge amplitude.

Let us consider the Regge parameters in the u channel. The Σ trajectory we use is given as [35]

$$\alpha_\Sigma(u) = -0.79 + 0.87u. \quad (22)$$

Since the QGSM is applicable only to the planar diagram [23,24], we cannot rely on it to determine the energy scale parameter $s_\Sigma^{\pi N:K\Lambda}$ in the u channel. Instead, we examine carefully a general phenomenological relation between the energy scale parameters (s_0) and the reaction thresholds (s_{th}), based on previous and present works in both the strangeness and charm sectors. Since we already know the values of s_0 in the t channel, we attempt to find a relation between s_0 and s_{th} by defining $s_0/\sqrt{s_{\text{th}}} = \beta$. Then, we get $s_{K^*}^{\pi N:K\Lambda}/\sqrt{s_{\text{th}}^s} = 1.0$ GeV and $s_{D^*}^{\pi N:D\Lambda_c}/\sqrt{s_{\text{th}}^c} = 1.1$ GeV ($s_{D^*}^{\pi N:D\Lambda_c}$ will be calculated in the next subsection), where $\sqrt{s_{\text{th}}^s} = M_K + M_\Lambda = 1.61$ GeV and $\sqrt{s_{\text{th}}^c} = M_D + M_{\Lambda_c} = 4.16$ GeV. Interestingly, the value of β is always kept to be around 1 GeV, being independent of a type of the reactions. For example, we find also $\beta\approx 1$ GeV for the $\bar{p}p\to\bar{\Lambda}\Lambda(\bar{\Lambda}_c^+\Lambda_c^+)$ and $\bar{p}p\to\bar{K}K(\bar{D}D)$ reactions [34]. Thus, it is reasonable to choose s_0 in such a way that the value of β is kept to be equal to 1 GeV. The energy scale parameters in the u channel are taken to be $s_\Sigma^{\pi N:K\Lambda}/\sqrt{s_{\text{th}}^s} = s_{\Sigma_c}^{\pi N:D\Lambda_c}/\sqrt{s_{\text{th}}^c} = 1.0$ GeV in the present calculation.

TABLE II. Vector-meson trajectories in the charm sector [33,34].

	$\alpha(0)$	$\sqrt{T}\times$ [GeV]	α'[GeV^{-2}]
$\bar{q}q(\rho)$	0.55	2.46	0.742
$\bar{c}q(D^*)$	−1.02	3.91	0.467
$\bar{c}c(J/\psi)$	−2.60	5.36	0.340

C. Charm production $\pi^- p\to D^-\Lambda_c^+$

We extend the study of the strangeness production to the charm production $\pi^- p\to D^-\Lambda_c^+$ just by substituting charm hadrons for the strangeness ones, i.e., $K\to\bar{D}$, $K^*\to\bar{D}^*$, $\Lambda\to\Lambda_c^+$, and $\Sigma^0\to\Sigma_c^+$. The D^*-meson trajectory in t-channel exchange can be found as in the case of the strangeness production. The relevant results are listed in Table II [33,34]. Equation (14) is also modified as

$$(s_{D^*}^{\pi N:D\Lambda_c})^{2(\alpha_{D^*}(0)-1)} = (s^{\pi N})^{\alpha_\rho(0)-1}\times(s^{D\Lambda_c})^{\alpha_{J/\psi}(0)-1}, \quad (23)$$

and we get $s^{\pi N}\simeq 1.5$ GeV^2, $s^{D\Lambda_c}\simeq 5.46$ GeV^2, and $s_{D^*}^{\pi N:D\Lambda_c}\simeq 4.748$ GeV^2. Lastly, the Σ_c trajectory is found to be

$$\alpha_{\Sigma_c}(u) = -2.23 + 0.532u, \quad (24)$$

as done similarly in Ref. [34] where the Λ_c trajectory was calculated to be $\alpha_{\Lambda_c}(u) = -2.09 + 0.557u$.

Note that for the scale factors in Eqs. (3) and (17) the same values will be used in this charm production to avoid ambiguity. We also consider the same values of the coupling constants for the corresponding vertices such that we can compare the magnitudes of the observables for the charm production with those for the strangeness production.

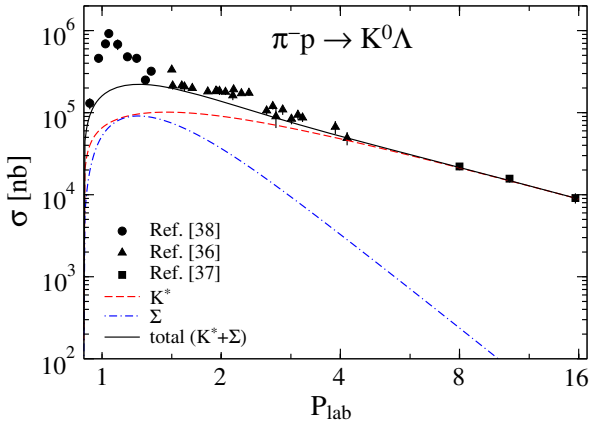

FIG. 2. Total cross section with each contribution is plotted as a function of $P_{\rm lab}$ for the $\pi^- p \to K^0\Lambda$. The experimental data are taken from Ref. [38] (circle), Ref. [36] (triangle), and Ref. [37] (square).

III. RESULTS AND DISCUSSION

Figure 2 shows the numerical results of the total cross section for the $\pi^- p \to K^0\Lambda$ as a function of $P_{\rm lab}$, which is the total momentum in the lab system. They are in good agreement with the experimental data at intermediate [36] and high [37] energies. On the other hand, the present results seem underestimated near threshold, compared with the data [38]. Note that the resonance contributions or the coupled-channel effects play a dominant role in explaining the data near threshold [22,39,40]. We do not take into account the nucleon resonances in the s channel in the present work, since we are mainly interested in studying the order of magnitude of the charm production in comparison with that of the strangeness production. As drawn in Fig. 2, the K^* and Σ Reggeons have comparable effects on the total cross section in the lower energy region. However, as $P_{\rm lab}$ increases, the contribution of the Σ falls off much faster than that of the K^*. Thus, the dependence of the total cross section on $P_{\rm lab}$ is mainly governed by the t-channel process. The reason can be found in the fact that the intercept of Regge trajectory $\alpha(0)$ for the K^* Reggeon is much larger than that for the Σ Reggeon.

In Fig. 3, we depict the results of the differential cross sections $d\sigma/d\Omega$ as functions of $\cos\theta$, given 20 different values of $P_{\rm lab}$. They are in good agreement

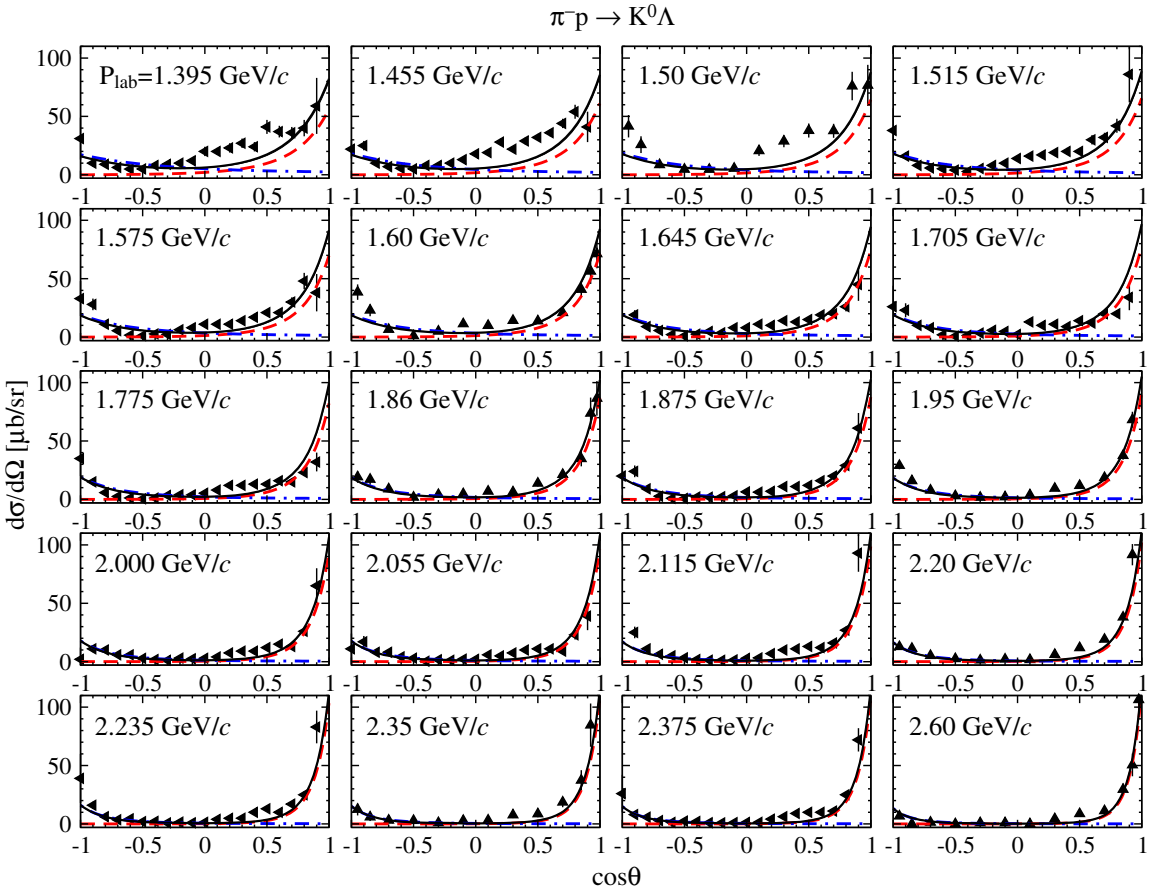

FIG. 3. Differential cross sections with each contribution are plotted as functions of $\cos\theta$ for the $\pi^- p \to K^0\Lambda$ in the range of 1.395 GeV $\le P_{\rm lab} \le$ 2.60 GeV. The experimental data are taken from Ref. [36] (triangle up) and Ref. [41] (triangle left). The notation is the same as Fig. 2.

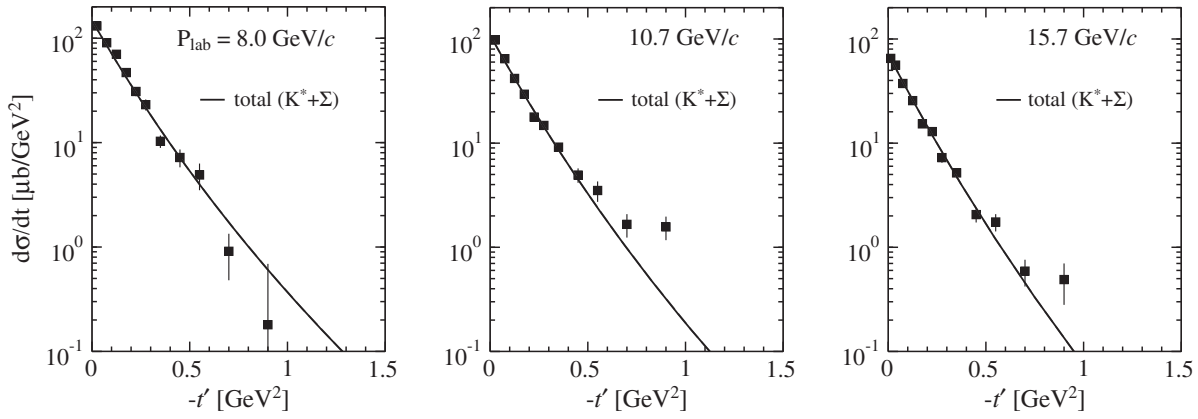

FIG. 4. Differential cross sections for the $\pi^- p \to K^0\Lambda$ are plotted as functions of $-t'$ at three different pion momenta ($P_{\rm lab}$). The experimental data are taken from Ref. [37].

with the experimental data [36,41], when $P_{\rm lab}$ is larger than 1.6 GeV. The discrepancy of our results from the data below 1.6 GeV arises from the same reason that we have not included the nucleon resonances in the s channel. Figure 4 displays the results of the differential cross section $d\sigma/dt$ as functions of $-t'$ defined as $t' = t - t_{\rm min}$, where $-t_{\rm min}$ represents the smallest kinematical value of $-t$ at fixed $P_{\rm lab}$. The results agree with the experimental data very well up to $-t' = 0.5$ GeV^2. We want to mention that K^* Reggeon exchange dictates the dependence of $d\sigma/dt$ on t'. In Fig. 5, we draw the results of the total cross section for the $\pi^- p \to D^-\Lambda_c^+$ as a function of $s/s_{\rm th}$ in comparison with that for the $\pi^- p \to K^0\Lambda$. Here the threshold value for the charm production is given as $s_{\rm th} = (M_D + M_{\Lambda_c})^2 = 17.3\,\text{GeV}^2$. Each contribution has a similar tendency as in the case of the $\pi^- p \to K^0\Lambda$. As $s/s_{\rm th}$ increases, the total cross section is almost controlled by the D^* Reggeon exchange. However, the magnitude of the total cross sections for the charm production is about 10^4–10^6 times smaller than that for the strangeness production. We find the similar results in the study of the $K^*\Lambda$ and $D^*\Lambda_c^+$ production reactions [21]. Both the intercept $\alpha(0)$ and energy scale parameter s_0 are crucial to determine the total cross section for a corresponding process. While $\alpha_{K^*}(0)$ is given as $\alpha_{K^*}(0) = 0.414$ as listed in Table I, $\alpha_{D^*}(0)$ is found to be -1.02 in Table II. This difference makes the total cross section fall off faster than that of the strange production as $s/s_{\rm th}$ increases. The suppression of the present result is also seen in Ref. [27] where a simplified Regge model is employed. It is found that the cross sections are sensitive depending on the values of the intercept and hadron mass. The most optimistic estimation suggested 0.5 nb at peak position with $\alpha_{D^*}(0) = -0.6$ [27], whereas the present work yields 4 nb.

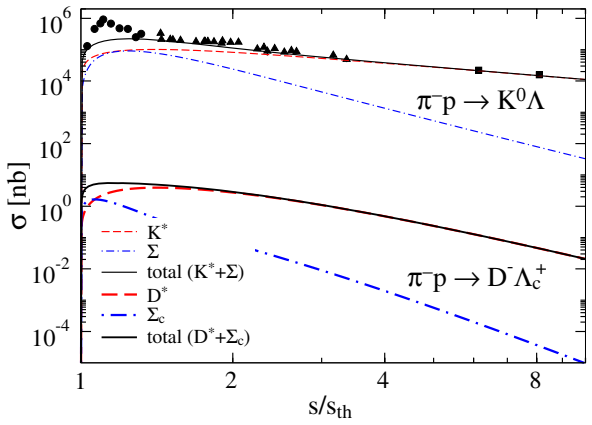

FIG. 5. Total cross section with each contribution is plotted as a function of $s/s_{\rm th}$ for the $\pi^- p \to D^-\Lambda_c^+$ in comparison with that for the $\pi^- p \to K^0\Lambda$. The experimental data are taken from Refs. [36–38].

Now we would like to check the uncertainties of the present results by using different sets of parameters. As mentioned already, we have employed the set ($\Lambda = 1$ GeV, $a_t = 0.40$, $a_u = 2.00$) for the charm production, which is determined from the strangeness sector. However, this is not a unique choice. Within a reasonable range of the cutoff Λ around 1 GeV, the parameter sets ($\Lambda = 1.2$ GeV, $a_t = 0.37$, $a_u = 1.80$) and ($\Lambda = 0.8$ GeV, $a_t = 0.45$, $a_u = 2.10$) can equally reproduce the strangeness production. When we apply these values to the charm production, the total cross sections lie in the range 1 nb–13 nb near threshold as shown in the left panel of Fig. 6. As the production energy increases, the difference becomes smaller gradually. It is worthwhile to compare our results with those from the other work [28] in which the same reaction $\pi^- p \to D^-\Lambda_c^+$ was investigated within a generalized parton picture, focusing on the reaction threshold and forward angle region. As shown in the right panel of Fig. 6, the results of this work lie

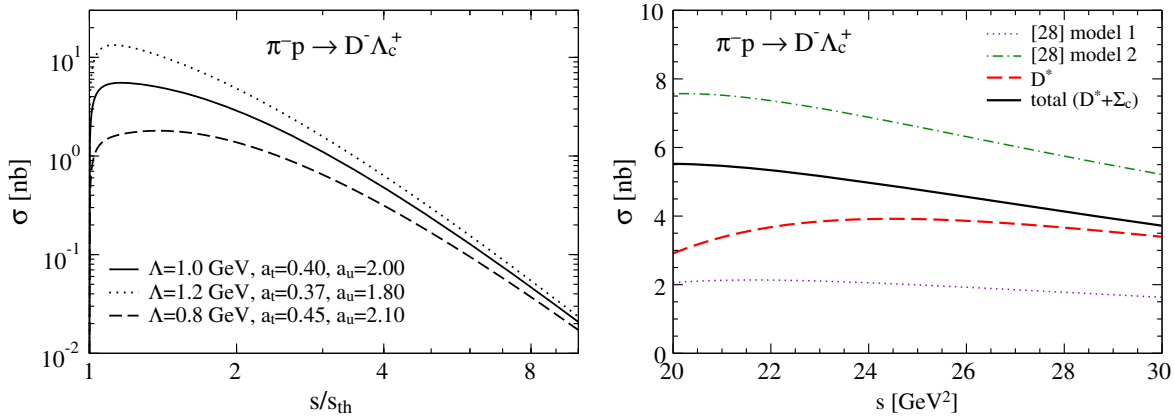

FIG. 6. Left panel: Total cross section for the $\pi^- p \to D^- \Lambda_c^+$ is plotted as a function of $s/s_{\rm th}$ with different parameter sets in the scale factors. Right panel: The present results are compared with those of Ref. [28] for the total cross section. The range of x-axis 20 GeV^2 $\leq$ $s \leq$ 30 GeV^2 corresponds to $1.2 \leq s/s_{\rm th} \leq 1.7$ in Fig. 5.

between those of model I and model II given in Ref. [28]. The s dependence of the present results look very similar to those of both model I and model II near threshold (20 GeV^2 $\leq s \leq$ 30 GeV^2). However, as s increases, the results of Ref. [28] fall off rather slowly [42], which deviates from the present ones. It indicates that the models developed in Ref. [28] do not satisfy the asymptotic behavior of the cross sections.

In Fig. 7, we continue to compare the present results of the differential cross sections $d\sigma/d\Omega$ with those of Ref. [28]. It is interesting to see that at forward angles both results are in good agreement with each other. However, the differential cross sections in backward angles were not considered in the models of Ref. [28]. Figure 8 illustrates the results of the differential cross sections $d\sigma/dt$ as functions of $-t'$ at three different values of $P_{\rm lab}$. The D^* Reggeon governs t' dependence

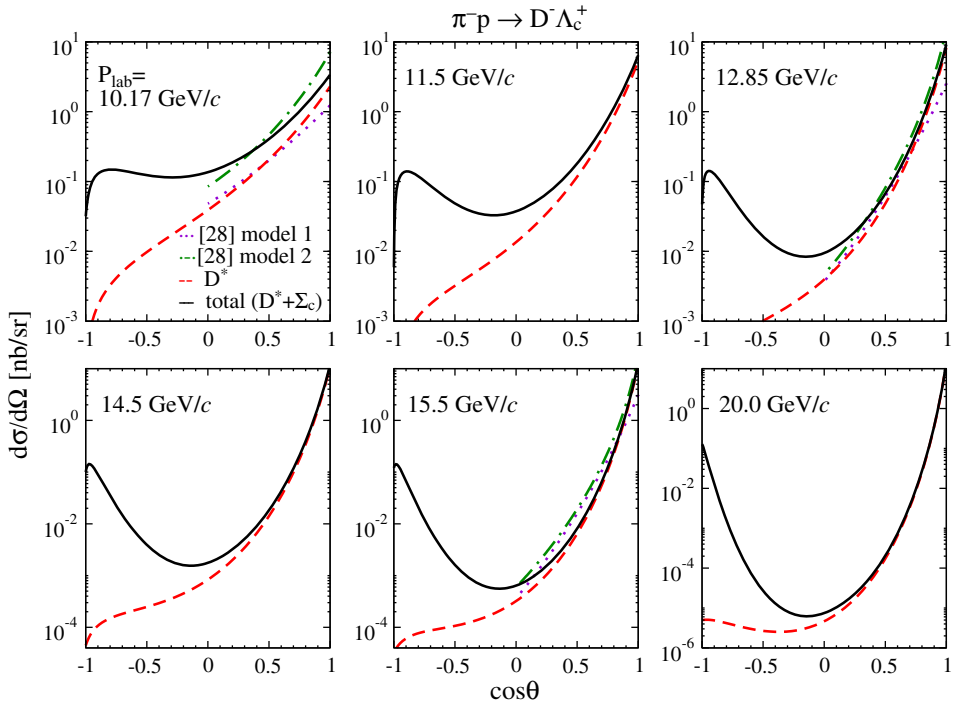

FIG. 7. Differential cross sections with each contribution are plotted as functions of $\cos\theta$ for the $\pi^- p \to D^- \Lambda_c^+$ at six different pion momenta ($P_{\rm lab}$). The present results are compared with those of Ref. [28].

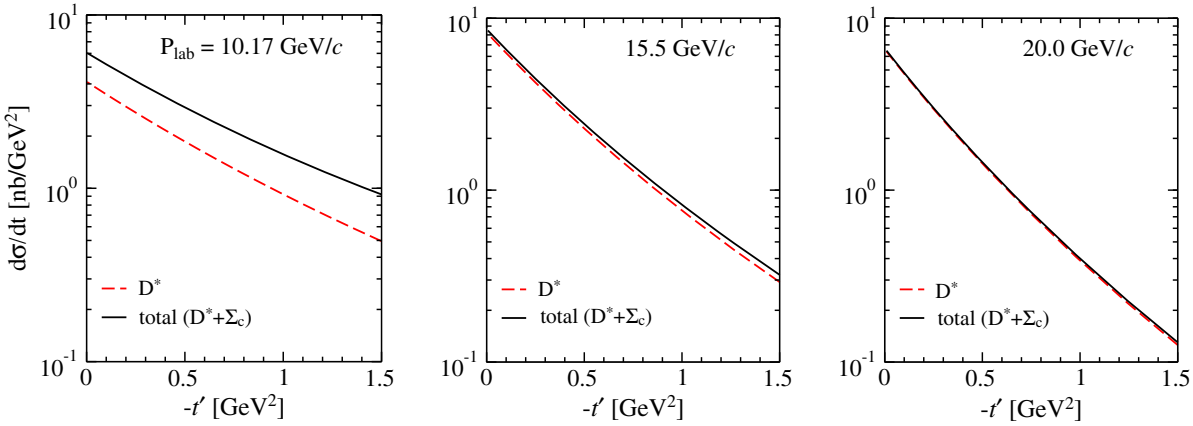

FIG. 8. Differential cross sections for the $\pi^- p \to D^- \Lambda_c^+$ are plotted as functions of $-t'$ at three different pion momenta ($P_{\rm lab}$).

at higher $P_{\rm lab}$, whereas the u channel has certain effects on the $d\sigma/dt$ near threshold.

IV. CONCLUSION AND SUMMARY

In the present work, we aimed at investigating the production mechanism of the $\pi^- p \to K^0 \Lambda$ and $\pi^- p \to D^- \Lambda_c^+$ reactions, based on a hybridized Regge model. We replaced the Feynman propagator by the Regge one from the invariant amplitudes. The Regge amplitudes explain the asymptotic behavior of the cross sections for the present reactions such that unitarity is well preserved, whereas the amplitudes from the effective Lagrangians correctly reproduce the magnitude of the cross sections near threshold. Combining each virtue of these two different approaches, we were able to study both the $K\Lambda$ and $D\Lambda_c$ productions consistently. Having determined the Regge parameters of K^* and D^* Reggeons by using the quark-gluon string model, and having fixed those of Σ and Σ_c Reggeons phenomenologically, we have computed the total cross sections, the differential cross sections $d\sigma/d\Omega$ and $d\sigma/dt$. As in the case of the $K^*\Lambda$ and $D^*\Lambda_c$ productions, we have found that the charm production is suppressed almost by similar order, i.e., the total cross sections for the charm production are 10^4–10^6 times smaller than those for the strangeness production depending on kinematical regions. We have compared the present results with those from the other work near the threshold region and at forward angles. Both results are qualitatively in agreement with each other.

Anticipating that the J-PARC, the BES-III, the JLAB, and the LHC facilities will produce a great deal of new experimental data related to charm physics, we find that it is of paramount importance to investigate the production mechanism of charmed hadrons with various probes. Relevant theoretical studies are under way.

ACKNOWLEDGMENTS

We are grateful to S. Kofler for sending us their results. This work was supported by the National Research Foundation of Korea (NRF) grant funded by the Korea government (MSIP) (No. NRF-2015R1A2A2A04007048). S. H. K. acknowledges the support of the Young Scientist Training Program at the Asia Pacific Center for Theoretical Physics from the Korea Ministry of Education, Science and Technology, Gyeongsangbuk-Do and Pohang City. A. H. acknowledges the support in part by Grant-in-Aid for Science Research (C) JP26400273 by the MEXT.

[1] E. S. Swanson, The new heavy mesons: A status report, Phys. Rep. **429**, 243 (2006).
[2] M. B. Voloshin, Charmonium, Prog. Part. Nucl. Phys. **61**, 455 (2008).
[3] N. Brambilla *et al.*, Heavy quarkonium: Progress, puzzles, and opportunities, Eur. Phys. J. C **71**, 1534 (2011).
[4] H. X. Chen, W. Chen, X. Liu, and S. L. Zhu, The hidden-charm pentaquark and tetraquark states, Phys. Rep. **639**, 1 (2016).
[5] S. K. Choi *et al.* (Belle Collaboration), Observation of a Narrow Charmonium-like State in Exclusive $B^\pm \to K^\pm \pi^+ \pi^- J/\psi$ Decays, Phys. Rev. Lett. **91**, 262001 (2003).
[6] B. Aubert *et al.* (*BABAR* Collaboration), Study of the $B \to J/\psi K^- \pi^+ \pi^-$ decay and measurement of the $B \to X(3872) K^-$ branching fraction, Phys. Rev. D **71**, 071103 (2005).
[7] B. Aubert *et al.* (*BABAR* Collaboration), Observation of a Broad Structure in the $\pi^+ \pi^- J/\psi$ Mass Spectrum around 4.26 GeV/c^2, Phys. Rev. Lett. **95**, 142001 (2005).

[8] K. Abe *et al.* (Belle Collaboration), Observation of a Charmoniumlike State Produced in Association with a J/ψ in e^+e^- Annihilation at $\sqrt{s} \approx 10.6$ GeV, Phys. Rev. Lett. **98**, 082001 (2007).

[9] S. K. Choi *et al.* (Belle Collaboration), Observation of a Resonance-Like Structure in the $\pi^{+-}\psi'$-prime Mass Distribution in Exclusive $B \to K\pi^{+-}\psi'$-prime Decays, Phys. Rev. Lett. **100**, 142001 (2008).

[10] A. Bondar *et al.* (Belle Collaboration), Observation of Two Charged Bottomonium-Like Resonances in Y(5S) Decays, Phys. Rev. Lett. **108**, 122001 (2012).

[11] M. Ablikim *et al.* (BESIII Collaboration), Observation of a Charged Charmoniumlike Structure in $e^+e^- \to \pi^+\pi^- J/\psi$ at $\sqrt{s} \approx 4.26$ GeV, Phys. Rev. Lett. **110**, 252001 (2013).

[12] Z. Q. Liu *et al.* (Belle Collaboration), Charmonium-Like State at Belle, Phys. Rev. Lett. **110**, 252002 (2013).

[13] M. Ablikim *et al.* (BESIII Collaboration), Observation of a Charged Charmoniumlike Structure $Z_c(4020)$ and Search for the $Z_c(3900)$ in $e^+e^- \to \pi^+\pi^- h_c$, Phys. Rev. Lett. **111**, 242001 (2013).

[14] R. Aaij *et al.* (LHCb Collaboration), Determination of the X(3872) Meson Quantum Numbers, Phys. Rev. Lett. **110**, 222001 (2013).

[15] R. Aaij *et al.* (LHCb Collaboration), Observation of the Resonant Character of the $Z(4430)^-$ State, Phys. Rev. Lett. **112**, 222002 (2014).

[16] S. Chatrchyan *et al.* (CMS Collaboration), Observation of a New Ξ_b Baryon, Phys. Rev. Lett. **108**, 252002 (2012).

[17] R. Aaij *et al.* (LHCb Collaboration), Observation of Two New Ξ_b^- Baryon Resonances, Phys. Rev. Lett. **114**, 062004 (2015).

[18] H. Noumi, Spectroscopic study of charmed baryons at J-PARC, *Proc. Sci.*, Hadron2013 (2013) 031.

[19] K. Shirotori *et al.*, Spectroscopy of charmed baryons at the J-PARC high-momentum beam line, J. Phys. Conf. Ser. **569**, 012085 (2014).

[20] S. H. Kim, A. Hosaka, H.-Ch. Kim, H. Noumi, and K. Shirotori, Pion-induced reactions for charmed baryons, Prog. Theor. Exp. Phys. (**2014**) 103D01.

[21] S. H. Kim, A. Hosaka, H.-Ch. Kim, and H. Noumi, Production of strange and charmed baryons in pion induced reactions, Phys. Rev. D **92**, 094021 (2015).

[22] D. Rönchen, M. Döring, F. Huang, H. Haberzettl, J. Haidenbauer, C. Hanhart, S. Krewald, U. -G. Meißner, and K. Nakayama, Coupled-channel dynamics in the reactions $\pi N \to \pi N$, ηN, $K\Lambda$, $K\Sigma$, Eur. Phys. J. A **49**, 44 (2013).

[23] A. B. Kaidalov, Hadronic mass relations from topological expansion and string model, Z. Phys. C **12**, 63 (1982).

[24] K. G. Boreskov and A. B. Kaidalov, Yad. Fiz. **37**, 174 (1983) [Production of charmed baryons in hadron-hadron collisions, Sov. J. Nucl. Phys. **37**, 100 (1983)].

[25] A. B. Kaidalov and O. I. Piskunova, Yad. Fiz. **43**, 1545 (1986) [Production of charmed particles in the quark-gluon string model, Sov. J. Nucl. Phys. **43**, 994 (1986)].

[26] A. B. Kaidalov and P. E. Volkovitsky, Binary reactions in anti-p p collisions at intermediate energies, Z. Phys. C **63**, 517 (1994).

[27] V. D. Barger and R. J. N. Phillips, Suppression factors in charmed particle production, Phys. Rev. D **12**, 2623 (1975).

[28] S. Kofler, P. Kroll, and W. Schweiger, $\pi^- p \to D^-\Lambda_c^+$ within the generalized parton picture, Phys. Rev. D **91**, 054027 (2015).

[29] K. A. Olive *et al.* (Particle Data Group), The Review of Particle Physics, Chin. Phys. C **38**, 090001 (2014).

[30] V. G. J. Stoks and Th. A. Rijken, Soft-core baryon-baryon potentials for the complete baryon octet, Phys. Rev. C **59**, 3009 (1999); Th. A. Rijken, V. G. J. Stoks, and Y. Yamamoto, Soft-core hyperon-nucleon potentials, ibid. **59**, 21 (1999).

[31] A. Donnachie, H. G. Dosch, P. V. Landshoff, and O. Nachtmann, *Pomeron Physics and QCD* (Cambridge University Press, Cambridge, UK, 2002).

[32] M. Guidal, J. M. Laget, and M. Vanderhaeghen, Pion and kaon photoproduction at high energies: Forward and intermediate angles, Nucl. Phys. **A627**, 645 (1997).

[33] M. M. Brisudova, L. Burakovsky, and J. T. Goldman, Effective functional form of Regge trajectories, Phys. Rev. D **61**, 054013 (2000).

[34] A. I. Titov and B. Kampfer, Exclusive charm production in $\bar{p}p$ collisions at $\sqrt{s} \lesssim 15$ GeV, Phys. Rev. C **78**, 025201 (2008).

[35] J. K. Storrow, Baryon exchange processes, Phys. Rep. **103**, 317 (1984).

[36] O. I. Dahl, L. M. Hardy, R. I. Hess, J. Kirz, D. H. Miller, and J. A. Schwartz, Strange-particle production in $\pi^- p$ interactions from 1.5 to 4.2 $\frac{\text{BeV}}{c}$. II: Two-body final states, Phys. Rev. **163**, 1430 (1967); Erratum, Phys. Rev.**183**, 1520(E) (1969).

[37] K. J. Foley, W. A. Love, S. Ozaki, E. D. Platner, A. C. Saulys, E. H. Willen, and S. J. Lindenbaum, Neutral associated production by 8-, 10.7-, and 15.7-$\frac{\text{GeV}}{c}\pi^-$ incident on protons, Phys. Rev. D **8**, 27 (1973).

[38] R. D. Baker, J. A. Blissett, I. J. Bloodworth, T. A. Broome, G. Conforto, J. C. Hart, C. M. Hughes, R. W. Kraemer *et al.*, The reaction $\pi^- p \to K^0\Lambda^0$ up to 1334 MeV/c, Nucl. Phys. **B141**, 29 (1978).

[39] H. Kamano, S. X. Nakamura, T.-S. H. Lee, and T. Sato, Nucleon resonances within a dynamical coupled-channels model of πN and γN reactions, Phys. Rev. C **88**, 035209 (2013).

[40] A. V. Anisovich, R. Beck, E. Klempt, V. A. Nikonov, A. V. Sarantsev, U. Thoma, and Y. Wunderlich, Study of ambiguities in $\pi^- p \to \Lambda K^0$ scattering amplitudes, Eur. Phys. J. A **49**, 121 (2013).

[41] D. H. Saxon, R. D. Baker, K. W. Bell, J. A. Blissett, I. J. Bloodworth, T. A. Broome, J. C. Hart, A. L. Lintern *et al.*, The reaction $\pi^- p \to K^0\Lambda^0$ up to 2375 MeV/c: New results and analysis, Nucl. Phys. **B162**, 522 (1980).

[42] Stefan Kofler (private communication).